# SUPPLEMENTAL EXPERIMETNAL PROCEDURES

**Mouse Strains and Cell Line**

LLO118αβ TCR transgenic (LLO118) mice have been described in our previous studies (Jiang et al., 2014). *Cd4-cre* mice (B6.Cg-Tg(*Cd4-cre*)1Cwi N9) were purchased from Taconic Labs. Strains with T cell-specific *Mir23a* deletion were generated by crossing *Mir23a*$^{f/f}$ mice with *Cd4-cre* mice. The LLO118-*Mir23a*$^{f/f}$*Cd4-cre* mice were generated from these three independent strains. All mice were bred and maintained in the specific pathogen-free facility managed by the Duke University Division of Laboratory Animal Research. FasL expressing L929 cell line was kindly provided by Dr. Youwen He.

**Antibodies**

Antibodies used were as follows: APC-Cy7 anti-mouse CD4 (GK1.5), PE-Cy7 anti-mouse CD4 (GK1.5), PE anti-mouse CD4 (GK1.5), Pacific Blue™ anti-mouse CD8a (53-6.7), APC anti-mouse CD8a (53-6.7), FITC anti-mouse CD8a (53-6.7), PE anti-mouse TCRβ (H57-597), PE-Cy7 anti-mouse TCRβ (H57-597), APC anti-mouse TCR Vα2 (B20.1), APC-Cy7 anti-mouse TCR Vα2 (B20.1), PE-Cy7 anti-mouse IFN-γ (XMG1.2), APC anti-mouse IFN-γ (XMG1.2), PE-Cy7 anti-mouse CD11b (M1/70), APC anti-mouse F4/80 (BM8), Pacific Blue™ anti-mouse Thy1.1 (OX-7), FITC anti-mouse Thy1.1 (OX-7), APC anti-mouse Thy1.2 (30-H12), PE-Cy7 anti-mouse Thy1.2 (30-H12), PE-Cy7 anti-mouse CD44 (IM7), PE-Cy5 anti-mouse CD44 (IM7), APC anti-mouse CD62L (MEL-14), PE anti-mouse CD62L (MEL-14), PE anti-mouse IL-2 (JES6-5H4) and APC anti-mouse IL-2 (JES6-5H4). All antibodies were purchased from Biolegend, CA, USA.

**Retrovirus Production**

Retrovirus was produced by transfecting 15μg of each retroviral vector in combination with 5μg pCL-Eco virus packaging vector into BOSC23 cells (from Dr. Garry Nolan Lab) using Lipofectamine® 2000 (Life Technologies, CA, USA). After 48h of transfection, the retrovirus-containing culture supernatant was collected for T cell transduction.

***Listeria* Colony Formation Unit (CFU) Assay**

Culture plate was made using BBL™ media (BD) with 1.5% agar. *Listeria* infected mice were sacrificed and one lobe of liver was collected for each animal. The livers were homogenized in 1ml of RPMI 1640. Next, 0.1ml of liver cells were precipitated and resuspended in 0.2ml water for passive lysis. 10μl lysate was used to make three 10-fold serial dilutions in water. 20μl of diluted liver cell lysate was plated on BBL agar plate. After overnight incubation in 37°C, *Listeria* CFU was quantified by colony counting.

**Bone Marrow Chimera Generation**

Bone marrow donors were first injected with 5-fluorouracil to enrich for progenitor cells. On day 7, total bone marrow cells were flushed from donor femur and tibia with RPMI 1640. Progenitor cells were purified using EasySep™ Mouse CD117 (cKit) Positive Selection Kit (Stemcell technologies). The cells were then cultured with X-VIVO culture media (Lonza) in the presence of 50ng/ml SCF, 10ng/ml IL-11 and 10ng/ml Tpo (Biolegend). After 24h of culture, cells were transduced with retrovirus. Fourty-eight hours later, virus-infected and linage negative cells were

sorted. *Tcra*$^{-/-}$ bone marrow recipients were given with 450 cGy irradiation and after two hours, the sorted progenitor cells were injected into the recipients intravenously.

**Modified Mitochondria Permeability Transition Assays**
$CD4^+$ T cells were stimulated using plate-bound anti-CD3ε and anti-CD28 antibodies (5μg/ml each) for 30min, in the presence of 10nM calcein and 500μM $CoCl_2$. After mitochondria were stained with MitoTracker® Deep Red (Life Technologies), cells were collected and analyzed by Amnis flow cytometry microscopy (EMD Millipore, MA, USA). The results were analyzed using the colocalization module of Amnis IDEAS software. Cells with co-localization between calcein staining and mitochondria staining were pre-gated, and the cellular median pixel intensity of calcein staining was quantified for each group. Representative images were generated by processing the calcein channel and MitoTracker® Deep Red channel with 2D-deconvolution (filter size 9, scaling factor 0.97, resulting scale 4) using MetaMorph software. The channels were merged and output was generated using FIJI software.

**Luciferase Assay**
The 3'UTR of predicted target genes were cloned into the pmirGLO Dual-Luciferase miRNA Target Expression Vector (Promega) which contains the reporter *Firefly* luciferase and control *Renilla* luciferase. The pmirGLO plasmid together with MSCV-MOCK or MSCV-miR23a plasmid was transfected into NIH-3T3 cell lines (ATCC). Forty-eight hours post-transfection, the luciferase activity of both *Firefly* luciferase and *Renilla* luciferase was measured with a Dual-Luciferase Reporter kit (Promega).

**Transmission Electron Microscopy**
TCR-stimulated cells were subsequently fixed in 10% glutaraldehyde and processed by The Shared Materials Instrumentation Facility at Duke University. Images were taken, in a double blinded way, under different magnifications by JEM-1400 TEM machine (JEOL, MA, US). Images under 1250×magnification were used for statistical analysis of the necrotic cells, images under 2050×magnification were used for representation of necrotic cell distribution, and images under 5600×magnification were used for visualization of mitochondria.

**microRNAome Analysis**
miRNA expression data was processed using the ExpressCluster module of the GenePattern program (http://cbdm.hms.harvard.edu/LabMembersPges/SD.html ), which was developed by Dr. Scott Davis in the Benoist/Mathis Lab (Harvard University). miRNA expression profiles across various stages of $CD4^+$ T cell responses were generated by unsupervised clustering using the K-Mean++ algorithm. Euclidean distance was selected as the distance metric, and the K-value (number of clusters) was set at 10 to avoid over-fitting and under-sitting.

**Target Ontology Enrichment Analysis**
Target ontology for miRNAs from the miRNA clusters were processed using the miRSystem online analysis tool (http://mirsystem.cgm.ntu.edu.tw/index.php) (Lu et al., 2012). For each miRNA, the human miRNA ortholog was requested for target prediction, and genes passing more than 3 prediction algorithms were added to the target list. Subsequently, the predicted target genes were subjected to Biocarta pathway ontology enrichment. The

BIOCARTA_G1_PATHWAY was used to score enrichment based on proliferation, and the BIOCARTA_DEATH_PATHWAY was used to score the enrichment based on cell death.

**Absolute Copy Number Quantification of miR-23a by RT-qPCR**

To ensure optimal miRNA extraction, RNA was isolated from cells using mirVana™ miRNA Isolation Kits (Thermo Fisher Scientific). Samples were then processed with Poly(A) Polymerase Tailing Kit (Epicentre) and cDNA was converted using qScript™ cDNA Synthesis Kit (Quanta Biosciences). For absolute quantification, plasmid containing miR-23a (MSCV-miR-23a) was used as standard. qPCR was performed on serial diluted MSCV-miR-23a plasmids and standard curve was generated for miR-23a. The same qPCR protocol was also applied to experiment samples and absolute copy numbers was converted from Ct values using the standard curve.

**shRNA Sequence for PPIF knockdown**

sh665: TGCTGTTGACAGTGAGCG CCTGTGGCCAGTTGAGCTAATC TAGTGAAGCCACAGATGTA GATTAGCTCAACTGGCCACAGT TGCCTACTGCCTCGGA.
sh710: TGCTGTTGACAGTGAGCG CGCAGGCATCCATGTCTTGATT TAGTGAAGCCACAGATGTA AATCAAGACATGGATGCCTGCT TGCCTACTGCCTCGGA.

**Table S1 (Supporting Figure 1)**. **Expression of miRNAs in CD4+ T cells from different stage of activation.** Purified naïve CD4+ T cells from LLO118 mice (LLO118-THY1.2+) were transferred into THY1.1+ recipient animals. Twenty-four hours post-cell transfer, mice were infected with 1×105 listeria. On day 0, day 3, day 5, day 7, day 14 and day 28 post-Listeria infection, donor cells were sorted from the recipients and the whole microRNAome was profiled by RT-qPCR. The Ct values were normalized to endogenous controls (U1,U6,RNY3,SNORD47) and converted to arbitrary units. The total miRNA data was categorized into 10 clusters using the ExpressCluster module. Details were shown in individual tabs.

## Supplementary Figures

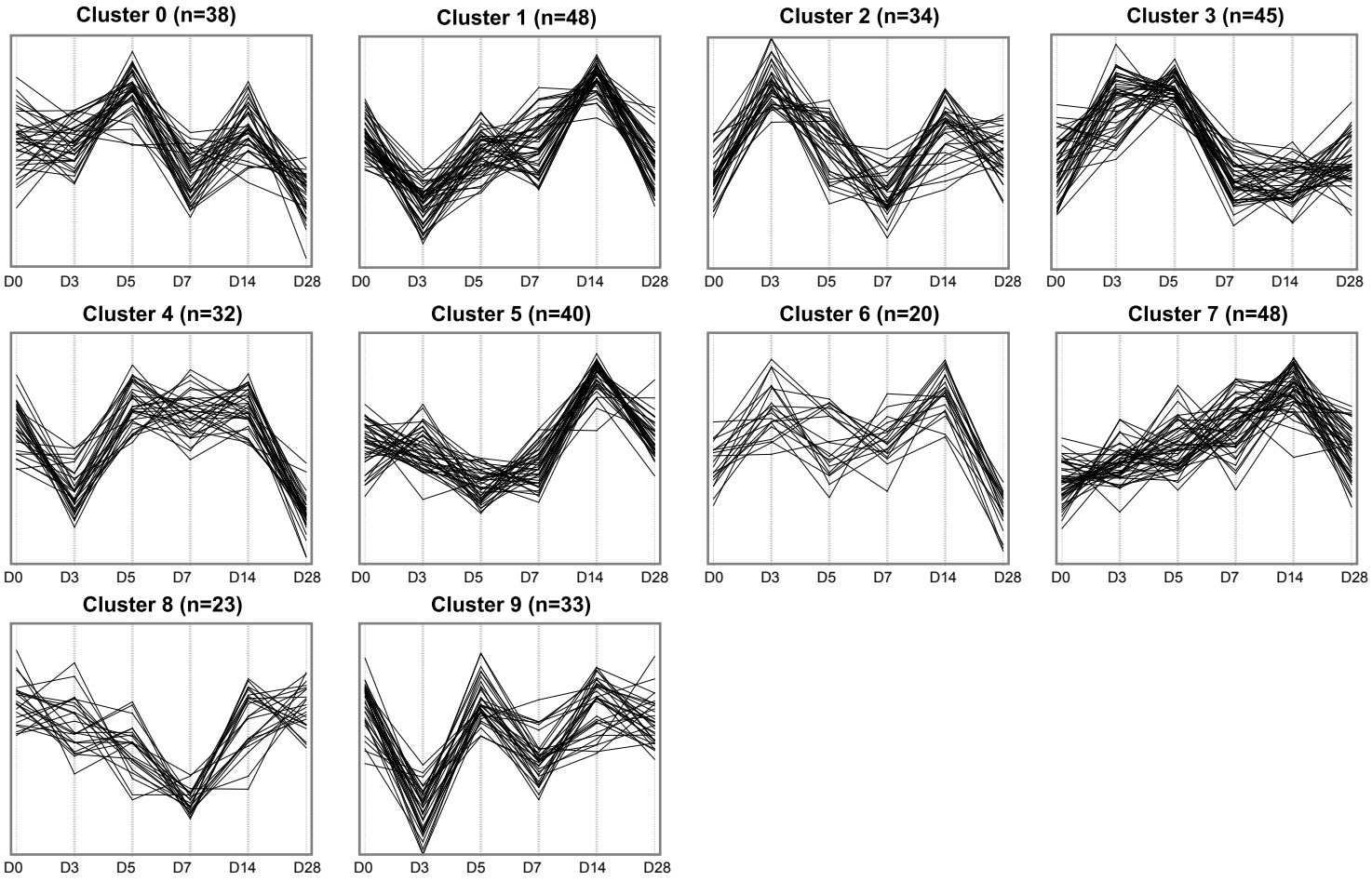


**Figure S1(Supporting Figure 1). Expression patterns of 361 miRNAs in CD4$^+$ T cells upon listeria infection.**

$2\times10^5$ Thy1.2$^+$ LLO118 TCRtg CD4$^+$ T cells were transferred into Thy1.1$^+$ recipients followed by $1\times10^5$ *Listeria* infection. On different time points, donor cells were sorted and miRNA expressions were measured by RT-qPCR. The expressions of the 361 miRNAs were assigned into 10 miRNA clusters by ExpressCluster as discussed in Supplemental Experimental Procedures.

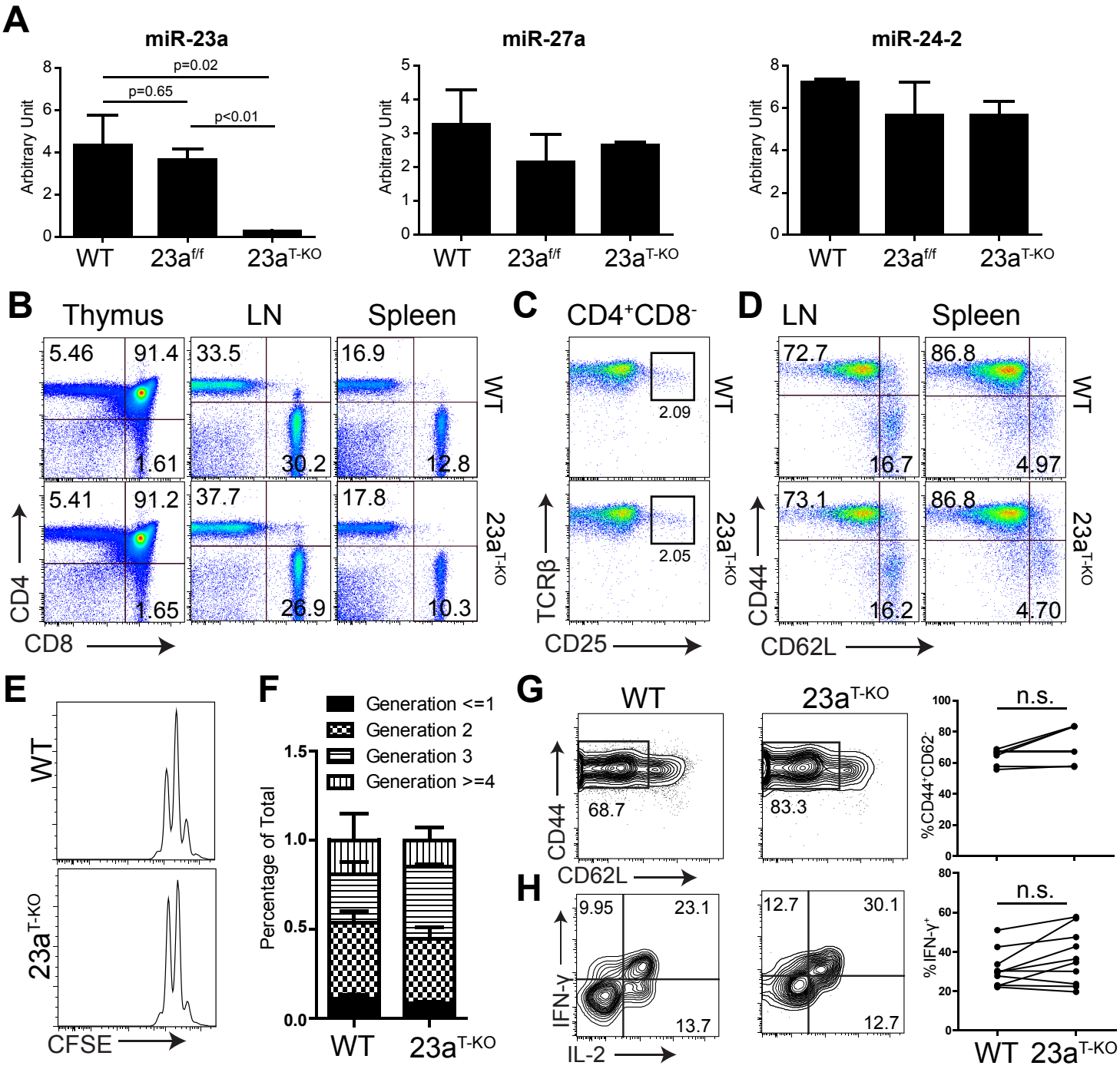


**Figure S2 (Supporting Figure 3). Normal development and activation of 23a$^{T\text{-}KO}$ T cells.**
(A) qPCR quantification of miR-23a, miR-27a and miR-24-2 expression in CD4$^+$ T cells from WT, 23a$^{f/f}$ and 23a$^{T\text{-}KO}$ animals. Data represents two independent experiments. (B) Percentage of CD4$^+$ and CD8$^+$ T cells in thymus, lymph nodes and spleens collected from naive WT and 23a$^{T\text{-}KO}$ mice. (C) Percentage of TCRβ$^+$CD25$^+$ Tregs in the thymus of WT and 23a$^{T\text{-}KO}$ mice. (D) CD44 and CD62L expression in CD4$^+$ T cells in the periphery. (E) Proliferation of CD4$^+$ T cells from WT and 23a$^{T\text{-}KO}$ upon TCR stimulation. CD4$^+$ T cells were isolated from WT and 23a$^{T\text{-}KO}$ mice, labelled by 5μM CFSE, and stimulated by plate-bound antibodies. Cell proliferation was measured by CFSE dilution. (F) Quantification of generation propagation as shown in (E). (G and H) Activation profile and cytokine expression of WT and 23a$^{T\text{-}KO}$ CD4$^+$ cells *in vivo*. LLO118 TCRtg WT and 23a$^{T\text{-}KO}$ cells were transferred into recipient animals followed by listeria infection as in Figure 3E. 4 days after infection, the activation status and cytokine production of transferred cells were measured by FACS.

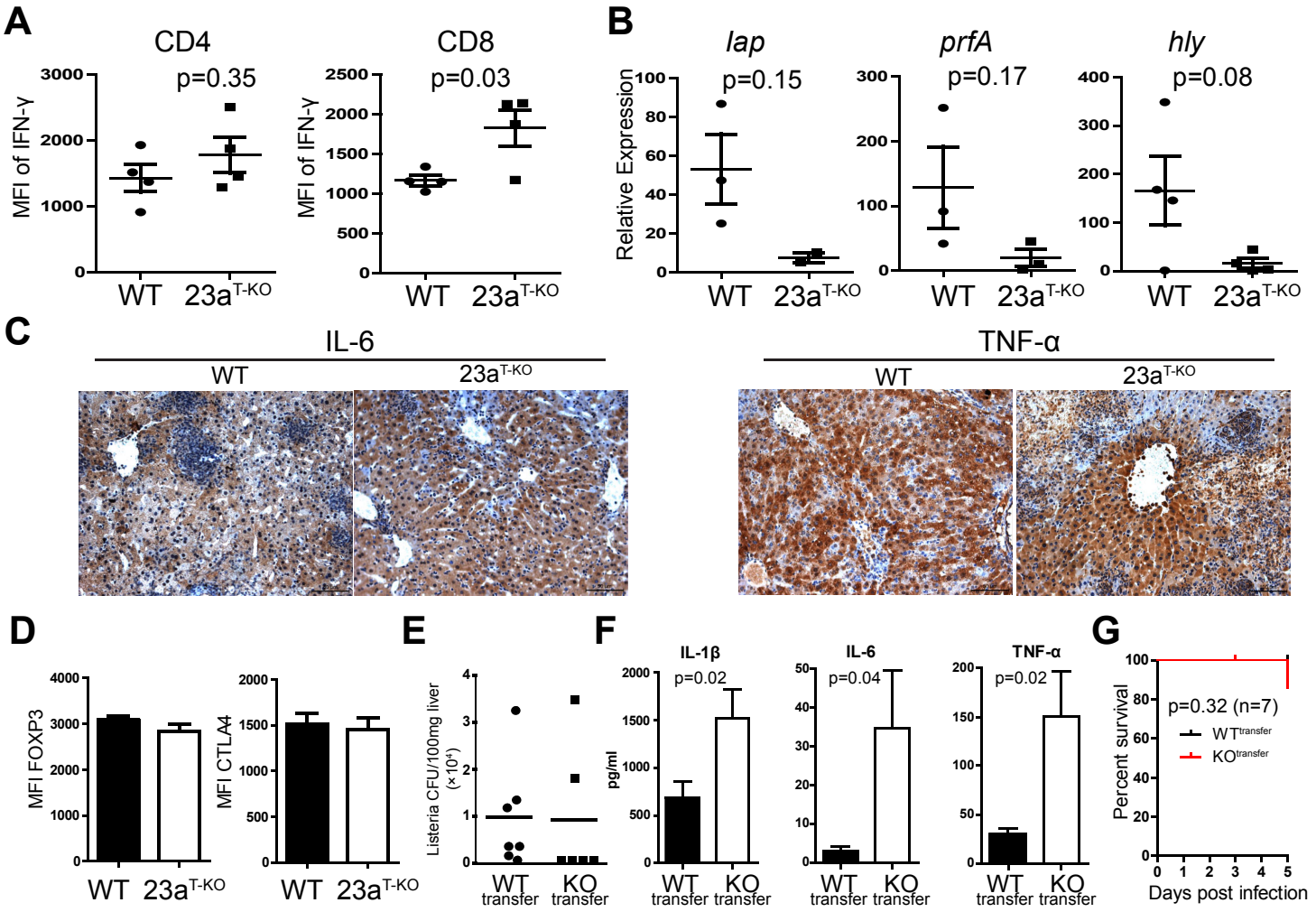


**Figure S3 (Supporting Figure 4). Characterization of WT and 23a$^{T\text{-}KO}$ mice after listeria infection.** WT and 23a$^{T\text{-}KO}$ mice were infected with 5x10$^5$ CFU listeria. Four days post infection, spleens and livers were collected for analysis. (A) IFNγ expressions in spleen CD4$^+$ and CD8$^+$ T cells. (B) Quantification of *Listeria*-specific genes in the liver of infected mice. Livers from infected WT and 23a$^{T\text{-}KO}$ mice were lysed for total RNA extraction. RT-qPCR was performed to quantify the *Listeria*-specific genes (*Iap*, *prfA* and *hly*) and the relative expression was normalized to β-Actin. (C) Immunohistochemistry staining of inflammatory cytokines in the infected liver. Liver tissues from infected mice were sectioned and stained for IL-6 and TNFα. (D) FOXP3 and CTLA4 expression in Treg cells. (E-G) TCRα$^{-/-}$ animals were transferred with 3×10$^6$ CD8$^+$ T cells purified from WT (WT$^{transfer}$) or 23a$^{T\text{-}KO}$ (KO$^{transfer}$) mice followed by 2×10$^5$ CFU *Listeria* infection. Recipient survival was tracked. (E) *Listeria* load in the liver of infected recipients and (F) Serum inflammatory cytokines in infected recipients were analyzed on day 5 post infection. (G) Survival curve of recipients with indicated CD8$^+$ transfers.

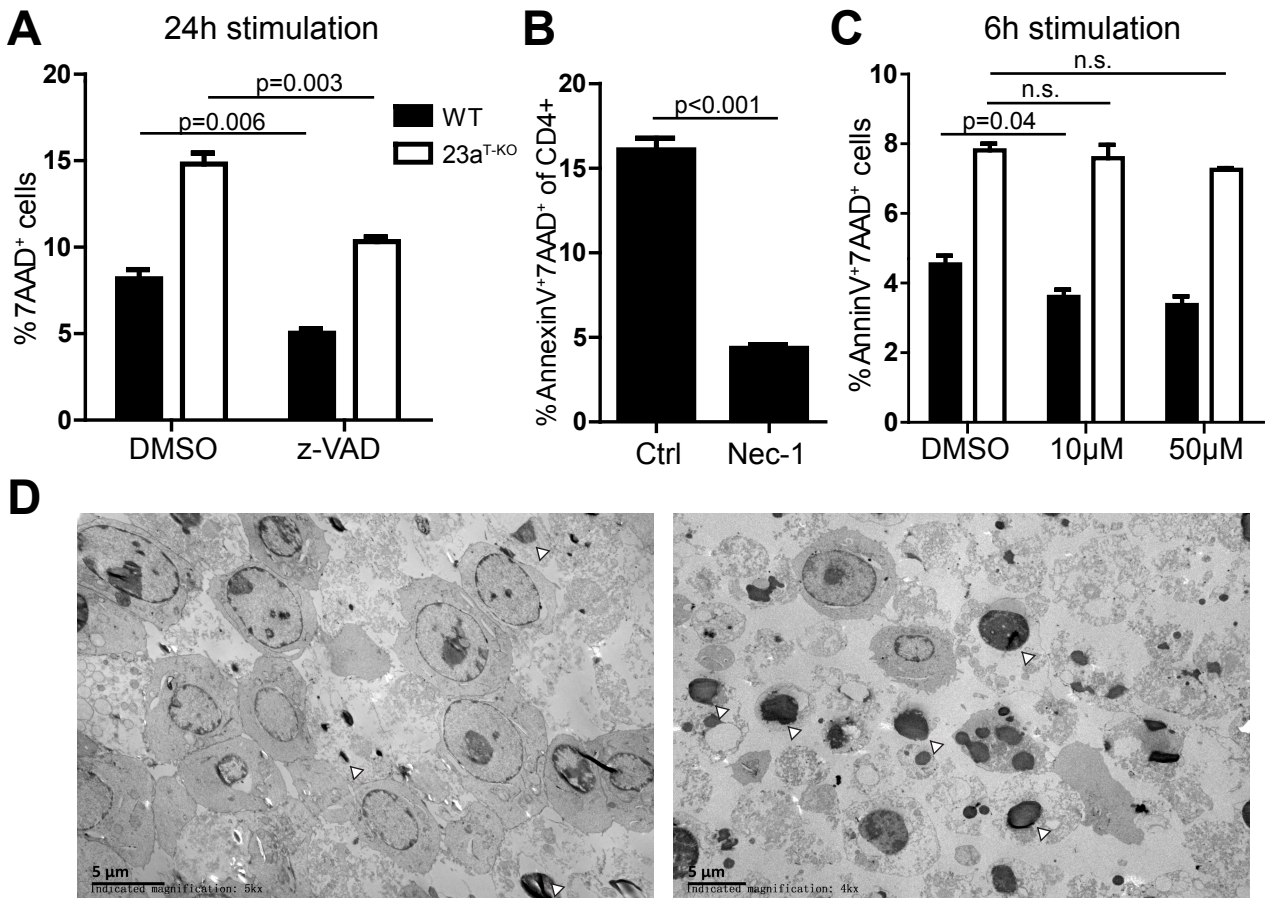


**Figure S4 (Supporting Figure 5). Characterization of 23a$^{T\text{-}KO}$ CD4$^{+}$ T cell death during *in vitro* activation.**

CD4$^{+}$ T cells were isolated from WT and 23a$^{T\text{-}KO}$ mice and stimulated by plate-bond antibodies. (A) Effect of caspase inhibitor on stimulated CD4$^{+}$ T cells. Cells were treated with DMSO or 10μM z-VAD-fmk and cultured for 24h. Cell death was measured by FACS. (B) Effect of Necrostatin-1 (Nec-1) on FasL+zVAD induced necrosis. CD4$^{+}$ T cells were cultured on FasL expressing feeder cells plus 20μM z-VAD-fmk for 24h and treated with DMSO or 50μM Nec-1. Cell death was measured by FACS. (C) Effect of RIP1 kinase inhibitor on stimulated CD4$^{+}$ T cells. Cells activated by plate-bound α-CD3 and α-CD28 and were treated with DMSO or different concentrations of Nec-1 for 6h. Cell death was measured by FACS. (D) TEM image of cells stimulated for 72h. Cells were cultured for 72h and cell morphology was imaged by TEM. Images were acquired under 4000x magnification. White arrows point to the apoptotic cells with condensed nuclei.

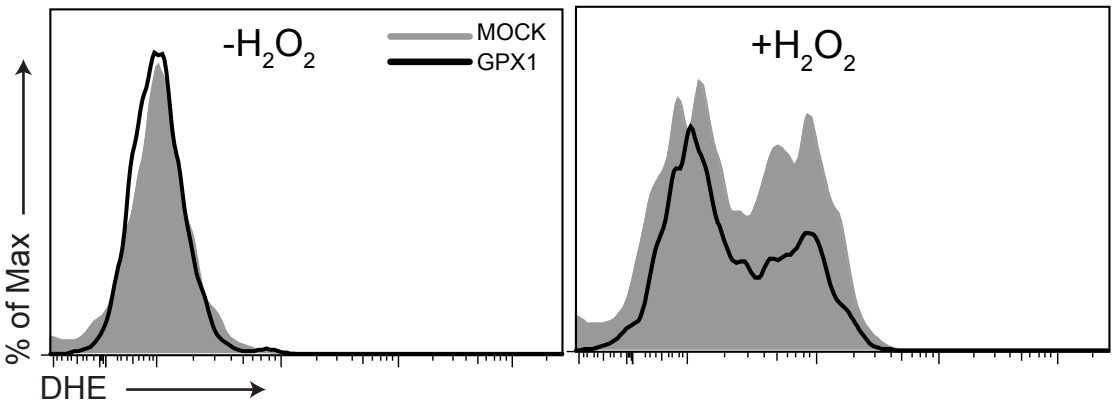


**Figure S5 (Supporting Figure 6). Antioxidation function of ectopically expressed GPX1.** HEK-293 cells were transfected with MSCV-MOCK or MSCV-GPX1 vectors. Forty-eight hours after transfection, cells were treated with or without 500μM $H_2O_2$ for 20min. Cellular oxygen free radicals were measured by DHE staining. The cells were pre-gated on $GFP^+$ population.

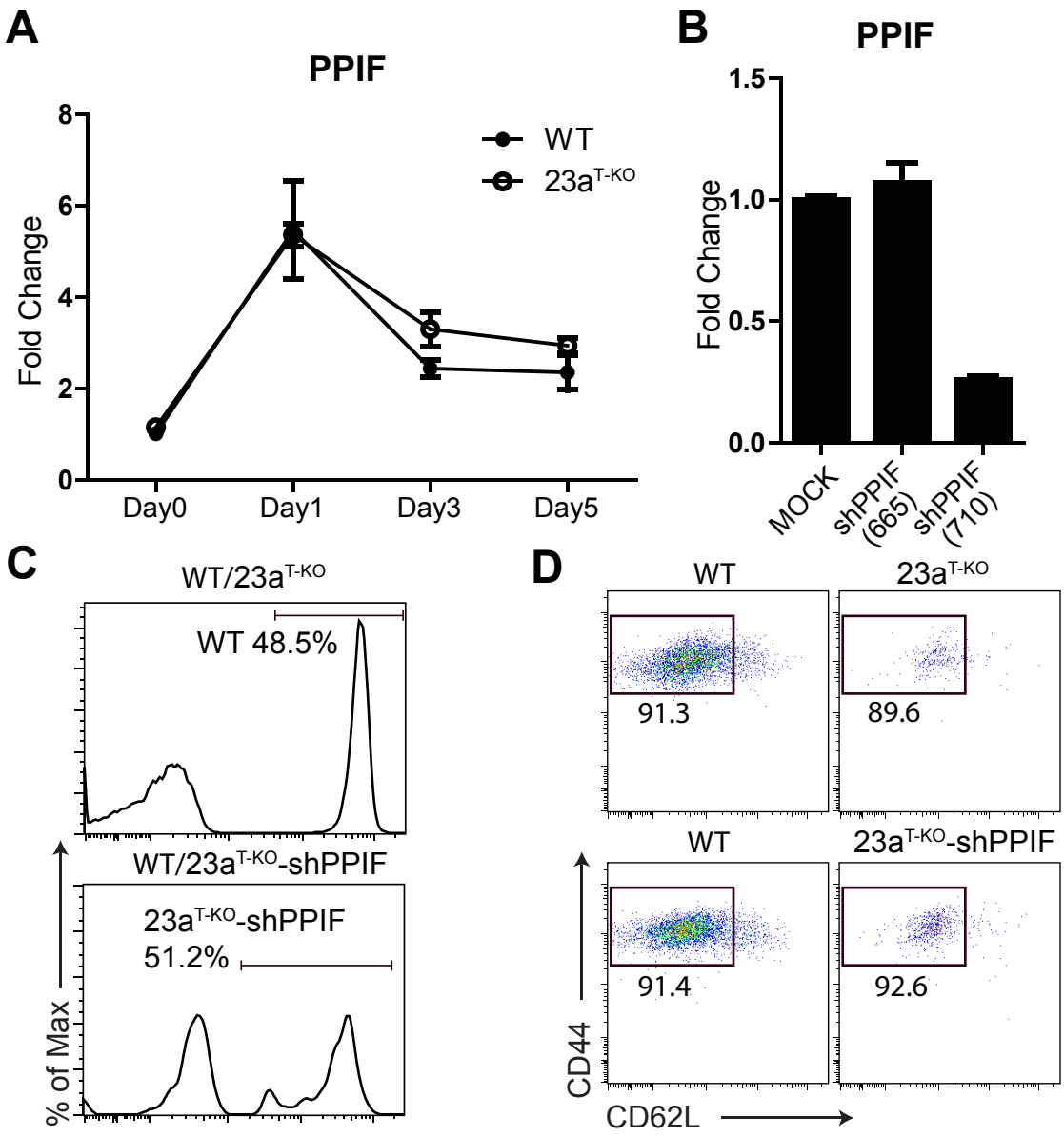


**Figure S6 (Supporting Figure 7). PPIF knockdown and in vivo adoptive transfer assays.** (A) PPIF expression after TCR stimulation. CD4$^+$ T cells from WT or 23a$^{T\text{-}KO}$ mice were activated by plate-bound α-CD3 and α-CD28. On different time points after activation, the expression of PPIF is quantified by RT-qPCR. (B) Knockdown efficiency of PPIF shRNA in CD4$^+$ T cells. Two PPIF targeting shRNA retroviral constructs shPPIF$_{665}$ and shPPIF$_{710}$ were designed. CD4$^+$ T cells from WT mice were activated and transduced with MOCK, shPPIF$_{665}$ and shPPIF$_{710}$ retrovirus. PPIF expression was quantified by RT-qPCR in different conditions. (C) FACS analysis of donor populations before transfer. In the competitive transfer experiment discussed in Figure 7, prior to injection, the WT/23a$^{T\text{-}KO}$ ratio or WT/23a$^{T\text{-}KO}$-shPPIF ratio were confirmed by flow cytometry. (D) Activation status of transferred cells after immunization. Seven days post immunization, the cell activation for corresponding donor populations were analyzed by CD44 and CD62L staining.